/N-39
51120
P-27

NASA Contractor Report 187211

Limit Pressure of a Circumferentially Reinforced SiC/Ti Ring

D.N. Robinson and M.S. Pastor
University of Akron
Akron, Ohio

October 1991

NASA
National Aeronautics and
Space Administration
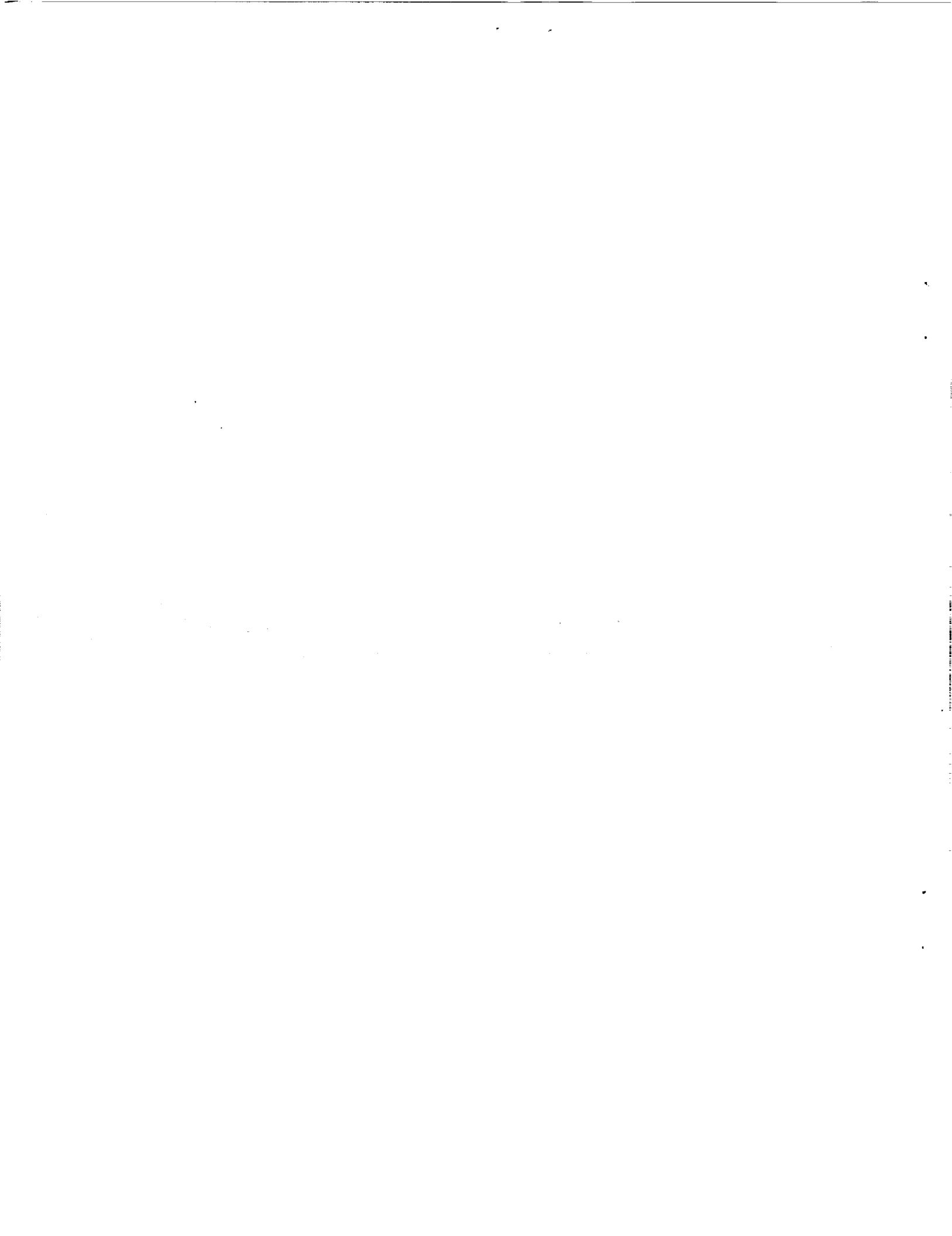
LIMIT PRESSURE OF A CIRCUMFERENTIALLY REINFORCED SiC/Ti RING

D.N.Robinson[1]and M.S.Pastor[2]
University of Akron
Department of Civil Engineering
Akron, Ohio 44325

ABSTRACT

Limit loads under plane stress and plane strain are found for a circumferentially reinforced elastic–plastic ring subjected to interior pressure. These are used as bounds on an estimate of the failure pressure of a SiC/Ti test ring that is being fabricated and tested under the co–sponsorship of NASA Lewis Research Center and Pratt and Whitney Aircraft. The ring is to serve as a benchmark against which deformation and failure analysis methods can be assessed. An anisotropic perfect plasticity idealization of the SiC/Ti ring material is made and used in the limit load calculations. An estimate of the failure pressure of the NASA/PW benchmark test ring is given.

---

[1] Prof., Univ. of Akron

[2] Grad. Student, Univ. of Akron

INTRODUCTION

A plastic limit analysis is made for estimating the failure pressure of a SiC/Ti test ring subjected to a monotonically increasing pressure at 427 C. The circumferentially reinforced SiC/Ti ring models a critical aircraft engine component. The fabrication and testing of the ring is co–sponsored by NASA Lewis Research Center and Pratt and Whitney Aircraft as a benchmark for assessing the applicability and accuracy of structural analysis and failure prediction methods for metallic composites.

Following Robinson and Duffy (1990) and Binienda and Robinson (1990), the SiC/Ti material is considered a pseudohomogeneous, locally transversely isotropoic continuum and is idealized as elastic perfectly plastic. The concepts of limit analysis of elastic–plastic continua are used under the assertion that strains large enough to cause rupture occur only as the plastic limit load P^l is reached (fig.1). This approach circumvents details such as residual stresses that affect the initial yield pressure P^y (fig.1) and the intermediate elastic–plastic response but not the limit pressure P^l. The failure pressure of the NASA/PW ring is bounded by calculating the limit pressures of the two limiting cases of plane stress and plane strain.

The objective is to provide an estimate of the failure pressure of the NASA/PW benchmark ring using approximate methods useful to the design engineer without conducting a detailed and costly structural analysis on a large computer. Limit analysis provides closed form expressions for the failure pressure, or bounds on it, valid for a range of ring geometries and material properties; such simple and flexible tools are useful to the designer, especially in the early stages of design. The limit load calculations also provide a check for verifying the correctness of a more comprehensive finite

element analysis of the NASA/PW ring.

The authors anticipate a sequel to this publication comparing the results obtained here with experimental results on the NASA/PW benchmark ring as they become available.

LIMIT ANALYSIS

We first state the anisotropic plasticity theory used in the analysis. Following Robinson and Duffy (1990), $d_i(x_j)$ is a unit vector field designating the local fiber direction (normal to the plane of transverse isotropy) at each material point. $D_{ij} = d_i d_j$ is a symmetric second rank orientation tensor. The yield function $\phi(\sigma_{ij})$ is

$$\phi(\sigma_{ij}) = J_2 - \frac{3}{4}\zeta I^2 - K^2, \tag{1}$$

written in terms of two invariants of the deviatoric stress s_{ij} and D_{ij}, viz,

$$J_2 = \frac{1}{2} s_{ij} s_{ji} \tag{2}$$

and
$$I = D_{ij} s_{ji} \tag{3}$$

The parameter $0 \leq \zeta \leq 1$ designates the degree of anisotropy. $\zeta = 0$ corresponds to full isotropy whereas $\zeta = 1$ indicates unlimited strength in the fiber direction. K is the yield stress under transverse shear.
The flow law is

$$\dot{\epsilon}_{ij} = \lambda \Gamma_{ij} \ (\lambda \geq 0) \quad \text{if } \phi = 0 \text{ and } \Gamma_{ij}\dot{\sigma}_{ji} = 0 \tag{4}$$

$$\dot{\epsilon}_{ij} = 0 \quad \text{if } \phi < 0 \text{ or } \phi = 0 \text{ and } \Gamma_{ij}\dot{\sigma}_{ji} < 0$$

in which
$$\Gamma_{ij} = s_{ij} - \frac{1}{2}\zeta I(3D_{ij} - \delta_{ij}) \tag{5}$$

3

Note that with $\zeta = 0$ this theory reduces to the classical J_2 (v.Mises) theory of a perfectly plastic solid.

Reduction of eqs.(1)–(5) to uniaxial stress gives

$$Y_l = K \sqrt{3/(1-\zeta)} \quad \text{and} \quad Y_t = K \sqrt{12/(4-\zeta)} \tag{6}$$

as the respective yield stresses along and transverse to the fiber direction.

In terms of cylindrical coordinates appropriate for the ring (fig.2) the nonzero stress components are σ_z, σ_c and σ_r. The inner and outer radii are denoted as a and b, respectively. Circumferential fiber reinforcement dictates that $D_{22} \equiv D_c = 1$, otherwise $D_{ij} = 0$.

The deviatoric stress components are

$$s_z = \frac{1}{3}[(\sigma_z-\sigma_r)+(\sigma_z-\sigma_c)]$$
$$s_c = \frac{1}{3}[(\sigma_c-\sigma_z)+(\sigma_c-\sigma_r)] \tag{7}$$
$$s_r = \frac{1}{3}[(\sigma_r-\sigma_c)+(\sigma_r-\sigma_z)]$$

and the components of Γ_{ij} are

$$\Gamma_z = s_z + \frac{1}{2}\zeta s_c$$
$$\Gamma_c = (1-\zeta)\, s_c \tag{8}$$
$$\Gamma_r = s_r + \frac{1}{2}\zeta s_c$$

In these terms, the yield function eq.(1) becomes

$$\phi = \frac{1}{2}(s_r{}^2 + s_z{}^2) - \frac{1}{4}(3\zeta-2)s_c{}^2 - K^2 \tag{9}$$

and the flow law is

$$\dot{\epsilon}_p = \lambda \Gamma_p \quad \text{if} \quad \phi = 0 \quad \text{and} \quad \Gamma_p \dot{\sigma}_p = 0 \tag{10}$$

$$\dot{\epsilon}_p = 0 \quad \text{if} \quad \phi < 0 \quad \text{or} \quad \phi = 0 \quad \text{and} \quad \Gamma_p \dot{\sigma}_p < 0$$

with $\qquad\qquad p = z, c, r$

The equilibrium equation relating σ_c and σ_r is

$$r \frac{d}{dr} \sigma_r = \sigma_c - \sigma_r \tag{11}$$

and the compatibility equation in rate form is

$$\frac{d}{dr}(r \dot{\epsilon}_c) = \dot{\epsilon}_r \tag{12}$$

Generally, compatibility must be satisfied by the total strain rates. However, at the limit load where the elastic strain rates vanish, eq.(12) must be satisfied by the plastic strain rate field.

We shall first consider the plane strain problem, i.e., $\dot{\epsilon}_z \equiv 0$. Using this condition in eqs.(7),(8) and (10) results in

$$\sigma_z = \left(\frac{2+\zeta}{4-\zeta}\right)\sigma_r + \left(\frac{2(1-\zeta)}{4-\zeta}\right)\sigma_c \tag{13}$$

Thus we can eliminate σ_z in eqs.(7) and in the yield function eq.(9) giving

$$\phi = \frac{1-\zeta}{4-\zeta} (\sigma_c - \sigma_r)^2 - K^2 = 0 \tag{14}$$

or $\qquad \sigma_c - \sigma_r = \pm \sqrt{\dfrac{4-\zeta}{1-\zeta}} \, K \tag{15}$

Fig.3 shows the yield surface, eqs.(15), in the dimensionless stress space $(\sigma_c/2K, \sigma_r/2K)$. Also shown is a typical stress profile a–b for pressure loading under plane strain; evidently, the positive root in eqs.(15) is the physically meaningful one. Combining this and the equilibrium eq.(11),

yields a separable differential equation in σ_r and r. This equation can be integrated from r = a to r = b, making use of the boundary conditions $\sigma_r(a) = -P^1$ and $\sigma_r(b) = 0$, to yield a *lower bound* on the (dimensionless) limit pressure $P^1/2K$ for plane strain, i.e.,

$$\frac{P^1}{2K} = \frac{1}{2}\sqrt{\frac{4-\zeta}{1-\zeta}} \ln\frac{b}{a} \tag{16}$$

So far, only equilibrium, the constitutive law and the boundary conditions are shown to be satisfied (*not compatibility*), restricting eq.(16) to be a lower bound on the limit pressure.

The dimensionless equilibrium stress field at the limit pressure is

$$\frac{\sigma_r}{2K} = -\frac{1}{2}\sqrt{\frac{4-\zeta}{1-\zeta}} \ln\frac{b}{r} \tag{17}$$

$$\frac{\sigma_c}{2K} = \frac{1}{2}\sqrt{\frac{4-\zeta}{1-\zeta}} (1-\ln\frac{b}{r}) \tag{18}$$

with $\sigma_z/2K$ given by eq.(13). Inserting this stress field in eqs.(7),(8) and (10) results in the associated plastic strain rate field

$$\dot{\epsilon}_z = 0$$

$$\dot{\epsilon}_c = \lambda(r)\, 2K \sqrt{\frac{1-\zeta}{4-\zeta}} = \frac{\lambda^1}{r^2} \tag{19}$$

$$\dot{\epsilon}_r = -\lambda(r)\, 2K \sqrt{\frac{1-\zeta}{4-\zeta}} = -\frac{\lambda^1}{r^2}$$

where, consistent with the perfect plasticity constitutive law, λ is taken as

$$\lambda(r) = \frac{1}{r^2} \quad \text{and} \quad \lambda^1 = 2K\sqrt{\frac{1-\zeta}{4-\zeta}} = \text{const.}$$

This strain rate field is seen to satisfy compatibility, eq.(12), thus elevating

6

eq.(16) to the *exact limit pressure for plane strain* under the present material idealization.

We now consider the plane stress problem in which $\sigma_z \equiv 0$. With this condition in eqs.(7), the yield condition eq.(1) becomes

$$\phi = \frac{1}{3}\left[(1-\zeta)\sigma_c^2 - (1-\zeta)\sigma_c\sigma_r + (1-\tfrac{\zeta}{4})\sigma_r^2\right] - K^2 \qquad (20)$$

At yield, $\phi = 0$, we can solve eq.(20) for σ_c giving

$$\sigma_c = \frac{1}{2}\left[\sigma_r \pm \sqrt{\beta(4K^2 - \sigma_r^2)}\,\right] \qquad ; \quad \sigma_r \leq 2K \qquad (21)$$

with $$\beta = \frac{3}{1-\zeta}$$

The yield surface, eq.(20), is shown in the dimensionless stress space $(\sigma_c/2K, \sigma_r/2K)$ of fig.4 for $\zeta = 0$ (isotropy), $\zeta = 0.977$ (used subsequently for the NASA/PW ring) and $\zeta = 1$ (the limiting case of infinite strength in the fiber direction). Also indicated in fig.4 is a typical stress profile a–b for a plane stress solution under pressure loading with $\zeta = .977$.

As for plane strain, the positive root in eqs.(21) is the physically meaningful one. It can be used to eliminate σ_c in the equilibrium eq. (11), again resulting in a differential equation in σ_r and r only. Integrating, as earlier, over $r = a$ to $r = b$ and invoking the boundary conditions $\sigma_r(a) = -P^l$ and $\sigma_r(b) = 0$, we obtain

$$\int_{-\frac{P^l}{2K}}^{0} \frac{2\,d\eta}{\sqrt{\beta\,(1-\eta^2)} - \eta} = \ln\frac{b}{a} \qquad ; \frac{P^l}{2K} \leq 1 \qquad (22)$$

as a *lower bound* on the (dimenionless) limit pressure $P^l/2K$ for plane

7

stress.

The dimensionless equilibrium stress field for plane stress is accordingly

$$\int_{\frac{\sigma_r}{2K}}^{0} \frac{2 \, d\eta}{\sqrt{\beta \, (1-\eta^2)} - \eta} = \ln \frac{b}{r} \qquad ; \frac{\sigma_r}{2K} \geq -1 \qquad (23)$$

with $\sigma_c/2K$ given by eq.(21) and $\sigma_z \equiv 0$.

Here, it is not such a simple matter to find an associated plastic strain rate field and show compatibility. However, we recognize that the strain rate field, eqs.(19), although not associated with the equilibrium plane stress field (eqs.(23) and (21)) through the constitutive law, is nevertheless *kinematically admissible* under plane stress and thus serves for establishing an *upper bound* on the limit pressure. This upper bound is obviously the limit load corresponding to plane strain, i.e., eq.(16).

Another upper bound on the limit load for plane stress is that corresponding to a local (*out of plane*) failure at the inner radius $r = a$ directly under the applied pressure. This upper bound is $P^l/2K = 1$, as is easily calculated using the kinematically admissible slip line field of fig.5. For this local mode to occur, the point on the stress profile corresponding to $r = a$ must be at C on the yield surface (fig.4). Point C ($\sigma_c/2K = -1/2$, $\sigma_r/2K = -1$) is independent of ζ and has an associated strain rate *vector* with components $\dot{\epsilon}_c = 0$ and $\dot{\epsilon}_r = -\dot{\epsilon}_z$.

Fig.6 is a plot of $P^l/2K$ vs. ζ for a pressurized ring in plane stress with $b/a = 1.8$, showing the lower bound, eq.(22), and the upper bounds, eq.(16) and $P^l/2K = 1$. For an isotropic material $\zeta = 0$, the limit pressure (fig. 6) is $P^l/2K \approx 0.58$. As the material is strengthened circumferentially,

the limit pressure increases ($P^l/2K \approx 0.84$ at $\zeta = 0.6$). The limit pressure continues to increase with increasing ζ until a *critical value* is reached (here, $\zeta \approx 0.8$) and the failure mode becomes one of local (*out of plane*) flow at $r = a$. Further circumferential strengthening is ineffective in increasing the limit pressure. As ζ increases beyond the critical value, the failure mode remains one of local flow with $P^l/2K = 1$; we refer to this condition as *over-reinforcement*. Analogous behavior is found by Lance and Robinson (1972) in other reinforced structures, e.g., beams, plates, etc. We note that the upper bound in fig.6 corresponding to eq.(16), i.e.,the exact limit load under plane strain, continues to increase with ζ , becoming infinite as $\zeta \to 1$. Thus, over-reinforcement in the sense discussed here does not occur under plane strain conditions.

The critical ζ in plane stress for a given b/a is obtained from eq.(22) by setting $P^l/2K = 1$. This is illustrated in the plot of b/a vs. ζ in fig.7. Alternatively, this graph can be interpreted as giving the *critical b/a ratio* at which the local (*out of plane*) failure mode takes effect for a given ζ. For *thick* rings with $b/a \geq$ the critical ratio, the ring fails locally at $r = a$ and $P^l/2K = 1$.

Fig.8 shows the yield surface in plane stress, eq. (20), for $\zeta = 0.8$. The stress profile a–b in fig.8 (solid curve) corresponds to the plane stress solution discussed above for $b/a = 1.8$. Note that point a (i.e., $r = a$) on the stress profile coincides with point C (cf.,fig.4), which, as remarked earlier, is a necessary condition for the local (*out of plane*) failure mode. The dotted curve in fig.8 represents a stress profile typical for $b/a < 1.8$, i.e., for a *thinner* ring.

We shall apply the results of these limit pressure calculations to the NASA/PW test ring in the following sections. However, first we characterize the SiC/Ti material using available experimental data.

CHARACTERIZATION OF SiC/Ti

The dotted curves in fig.9 represent longitudinal and transverse tensile data on SiC/Ti at 427 C. The solid curves are the perfect plasticity idealizations of these data used in the subsequent limit pressure calculations. The yield stress in the fiber direction Y_l is taken as being coincident with the fracture strength in that direction, viz., $Y_l = 200$ ksi. Two values are taken for the transverse yield strength, $Y_t = 30$ ksi and $Y_t = 35$ ksi delimiting a range of possible idealizations.

The material parameters ζ and K corresponding to these choices of yield stress are obtained through eqs.(6) and are shown in the following table (Y_l, Y_t and K are in ksi):

Table 1

Y_l	Y_t	ζ	K
200	30	.983	15.04
200	35	.977	17.56

APPLICATION TO THE NASA/PW TEST RING

The NASA/PW ring has a circumferentially reinforced SiC/Ti core covered with a layer of Ti cladding. Fig.10 shows the dimensions of the cross section and the relevant radii. Limit load calculations are made for two ring geometries (a and b are in inches), viz.,

Table 2

b	a	b/a
3.21	2.78	1.155
3.25	2.74	1.186

10

The first, b/a = 1.155 corresponds to the actual radii of the SiC/Ti core. This calculation ignores the presence of the cladding, taking the strength of the ring to result entirely from the reinforced core. The second calculation, b/a = 1.186 incorporates *effective* radii (b ≈ 3.25 and a ≈ 2.74) as a means of approximating the small contribution of strength of the Ti cladding. Here, the choice of radii amounts to enlarging the core dimensions by about one third of the cladding thickness. A more prudent choice must come from engineering experience based on experimental observation.

Critical values of ζ, delimiting local failure in plane stress (fig.7), are $\zeta = .992$ and $.989$ for b/a = 1.155 and 1.186, respectively. As each of these values exceeds $\zeta = .977$ and $.983$, identified in table 1 for the NASA/PW ring, we are assured that local failure is not a consideration here.

Plots of $P^l/2K$ vs. ζ for b/a = 1.155 and 1.186 are shown in figs.(11) and (12), respectively. In each case, the dotted (upper) curve represents the exact limit pressure for plane strain and the upper bound for plane stress (eq.(16)). As discussed earlier, the upper bound $P^l/2K = 1$ relating to local flow at r = a does not play a role here. The solid (lower) curve in each of the figs. (11) and (12) is the lower bound for plane stress (eq.(22)). Specific values of the limit pressure for plane strain P^l_e and the lower bound for plane stress P^l_s corresponding to ζ and K in Table 1 and the ratios b/a in Table 2 are calculated as (K, P^l_s and P^l_e are in ksi):

Table 3

ζ	K	b/a	P^l_s	P^l_e
.983	15.04	1.155	<u>25.3</u>	28.8
.977	17.56	1.155	26.5	<u>29.0</u>
.983	15.04	1.186	<u>28.1</u>	34.2
.977	17.56	1.186	30.1	<u>34.4</u>

11

Table 3 indicates bounds on the limit pressure for b/a = 1.155 as
25.3 ksi $\leq$ P^l $\leq$ 29.0 ksi, spanning $\pm$ 7% about an average of 27.15 ksi.
Recalling that b/a = 1.155 implies the strength of the ring is attributable
solely to the SiC/Ti core, we anticipate these bounds might tend to
underestimate the strength of the NASA/PW ring.

Bounds for b/a = 1.186 (in which limited strength of the cladding is
accounted for through specifying *effective* radii) are
28.1 ksi $\leq$ P^l $\leq$ 34.4 ksi. These range $\pm$ 10% about an average of
31.25 ksi. The lesser value 28.1 ksi corresponds to the lower bound for
plane stress with a transverse yield strength of Y_t = 30 ksi (fig.9); the
greater value 34.4 ksi relates to plane strain with Y_t = 35 ksi. The
authors submit these bounds as their best estimate of the failure pressure of
the NASA/PW benchmark ring at 427C.

CONCLUSIONS

The following accomplishments and conclusions are made in this
study:

• The limit load is found for a circumferentially reinforced
elastic–plastic ring (cylinder) subjected to interior pressure and in a
condition of plane strain.

• Upper and lower bounds on the limit load are found for a reinforced
ring (disc) under conditions of plane stress.

• These closed form solutions apply for all values of the material
parameters $0 \leq \zeta \leq 1$ and K (designating the degree of reinforcement and
the yield stress in transverse shear, respectively), and any b/a (ratio of
outer to inner radius). The results provide simple and useful tools for the
engineer designing fiber reinforced metallic rings.

- As $\zeta \to 1$ the limit pressure of the circumferentially reinforced ring in plane strain increases indefinitely. Conversely, the limit pressure of the ring in plane stress is bounded by its transverse ($\approx$ *matrix*) strength, ultimately failing by local plastic (*out of plane*) flow directly under the applied pressure.

- The limit load calculations are applied to the NASA/PW SiC/Ti test ring giving an estimated range of the failure pressure at 427 C of $\approx 28 - 34$ ksi.

- The calculated bounds on the limit pressure are useful in providing a check on more comprehensive finite element analyses.

ACKNOWLEDGEMENT

REFERENCES

Binienda,W.K. and Robinson,D.N. (1990). "Creep Model for Metallic Composites Based on Matrix Testing", *J.Engrg.Mech.*,117(3).

Lance,R.H. and Robinson,D.N. (1972). "Limit Analysis of Ductile Fiber–Reinforced Structures", *J.Engrg.Mech.Div.,ASCE*,98,EM1.

Robinson,D.N. and Duffy,S.F. (1990). "Continuum Deformation Theory for High Temperature Metallic Composites", *J.Engrg.Mech.*,116(4).
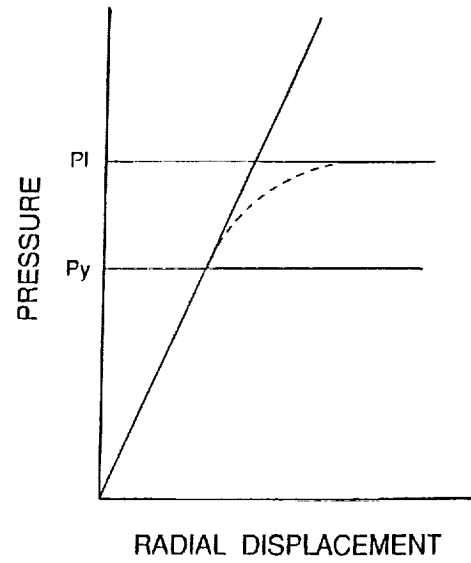
Fig.1 Schematic diagram of pressure vs. radial displacement.
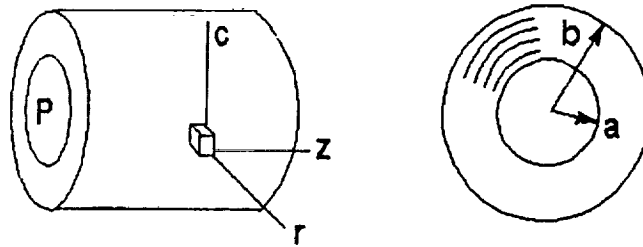
Fig.2 Cylindrical geometry (z,c,r) of circumferentially reinforced ring. b = outer radius, a = inner radius.
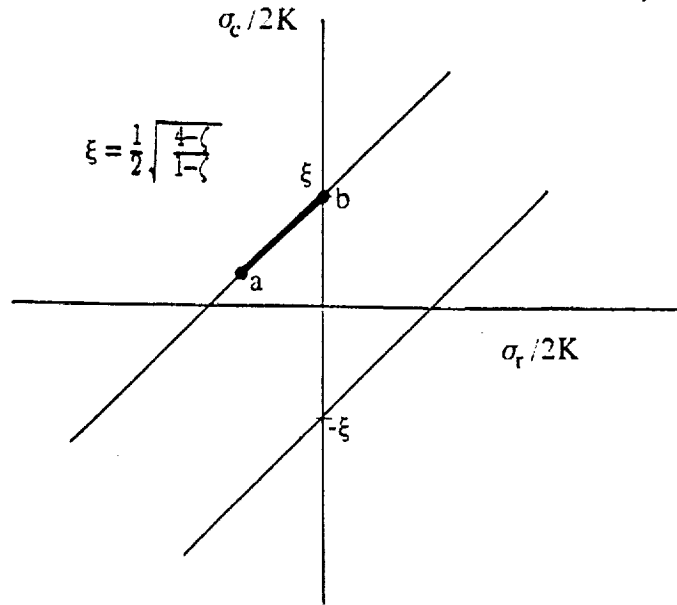
Fig.3 Yield surface for plane strain in the dimensionless stress space $\sigma_r/2K, \sigma_c/2K$. Typical stress profile a–b ($r=a \to r=b$) for pressure loading.
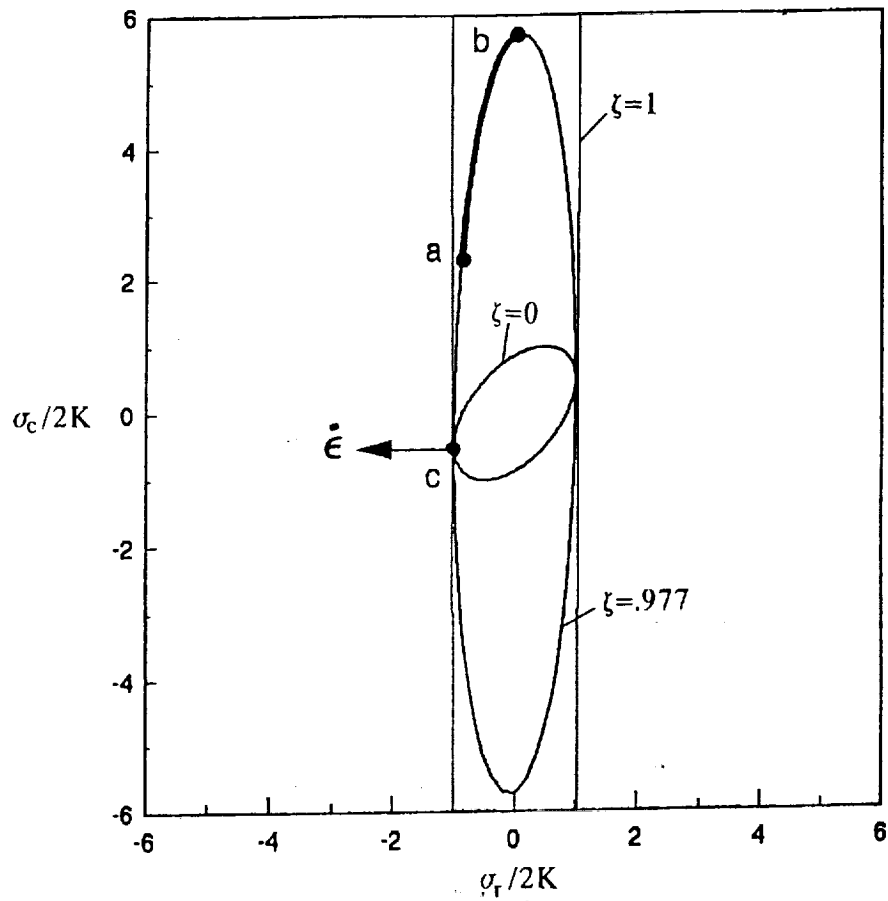
Fig.4 Yield surfaces for plane stress in $\sigma_r/2K, \sigma_c/2K$ space. Surfaces are shown for $\zeta = 0$, $\zeta = .977$ and $\zeta = 1$. Typical stress profile a–b for pressure loading with $\zeta = .977$.
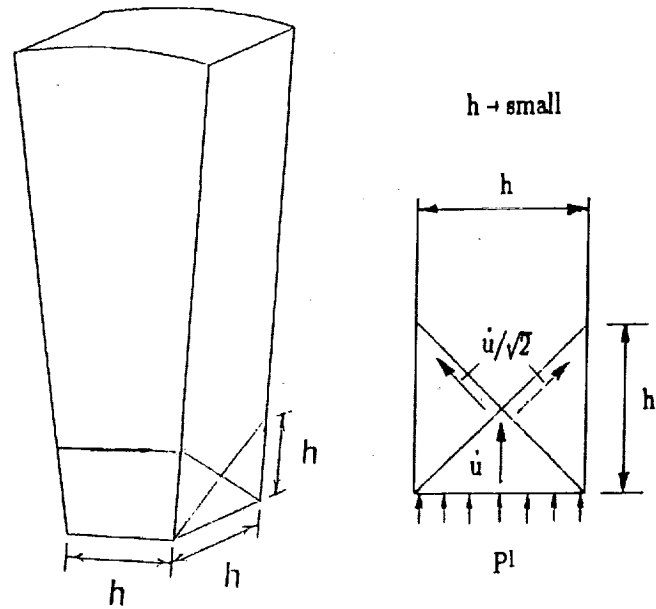
$$P^l h^2 \dot{u} = 4[(\dot{u}/\sqrt{2})(\sqrt{2}h/2)(h)(K)]$$

$$P^l/2K = 1$$

Fig.5 Kinematically admissible slip line field for local (out of plane) flow at $r = a$. Upper bound calculation giving $P^l/2K = 1$.
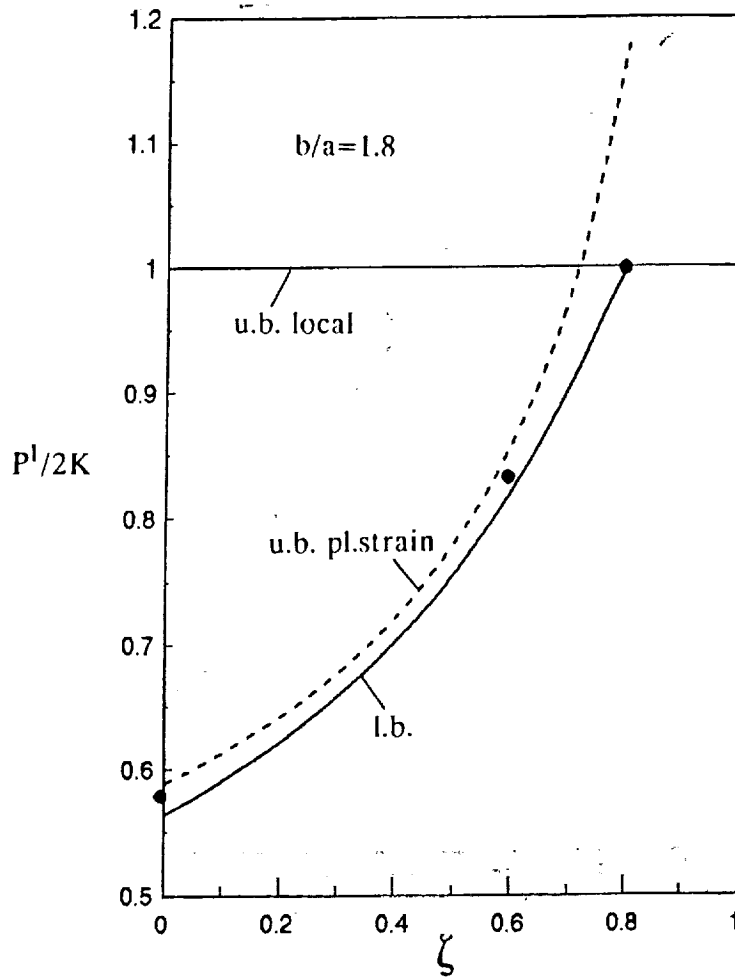
Fig.6 $P^l/2K$ vs. ζ for a pressurized ring in plane stress with $b/a = 1.8$. Lower bound, eq.(22), and upper bounds, eq.(16) and $P^l/2K = 1$. Critical $\zeta \approx 0.8$.
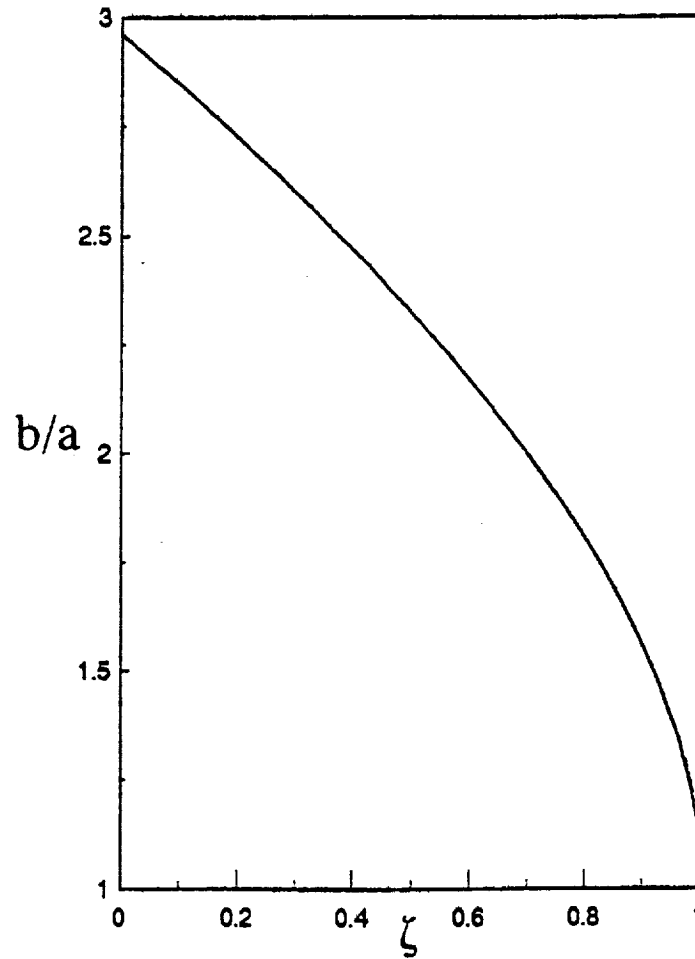
Fig.7 b/a vs. ζ for local (out of plane) failure in plane stress. $P^l/2K = 1$.
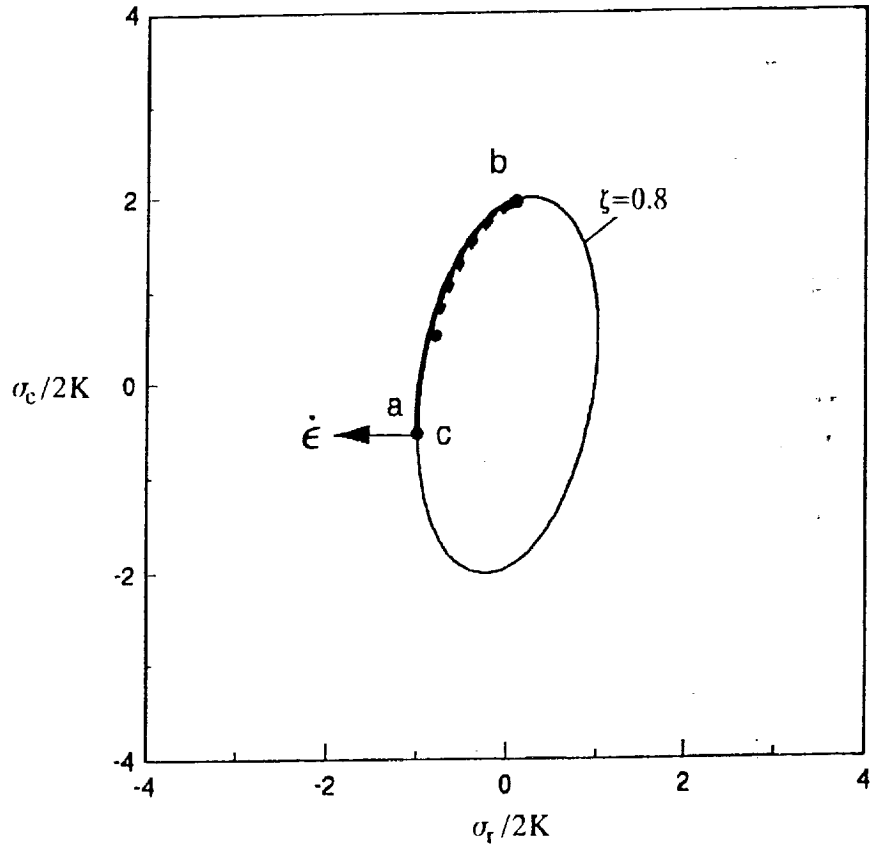
Fig.8 Yield surface in plane stress with $\zeta = 0.8$. Stress profile a–b (solid curve) for $b/a = 1.8$. Typical stress profile (dotted) for $b/a < 1.8$.
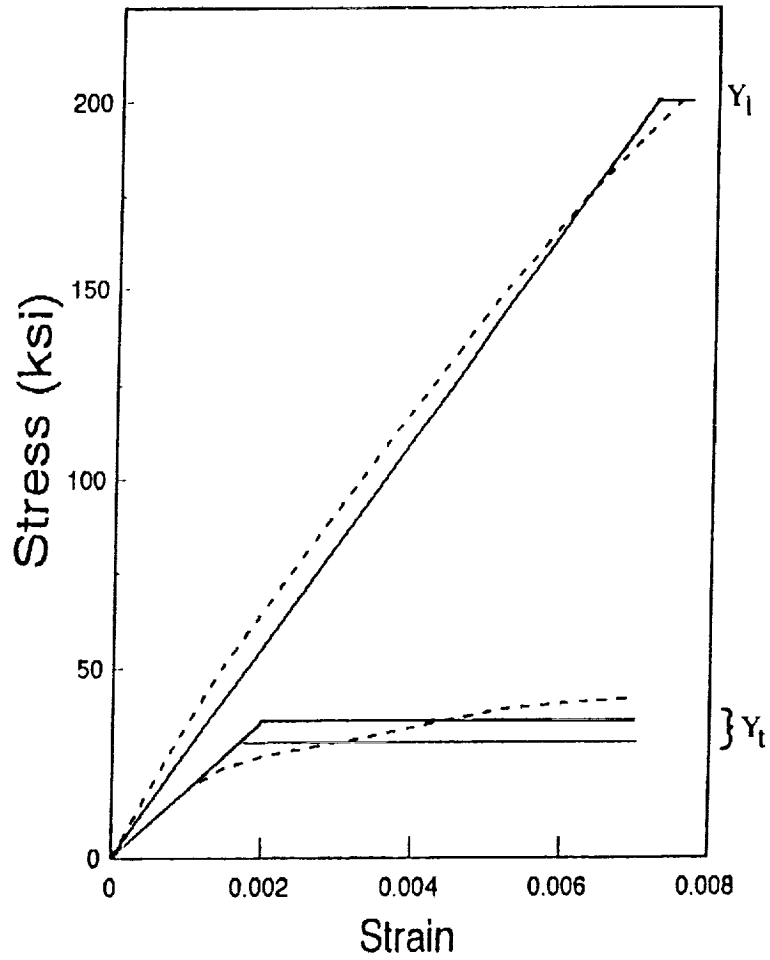
Fig.9 Longitudinal and transverse tensile curves (dotted) for SiC/Ti at
427 C. Elastic perfectly plastic idealizations (solid curves) indicating
Y_l and Y_t.
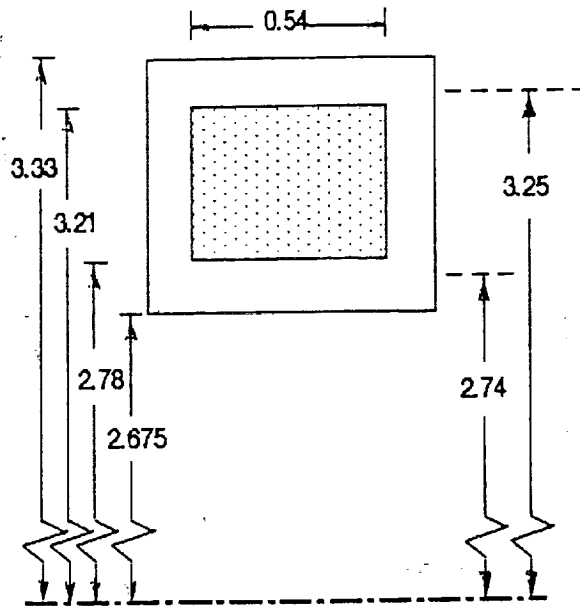
Fig.10 Cross section of NASA/PW test ring. Actual and *effective* radii.
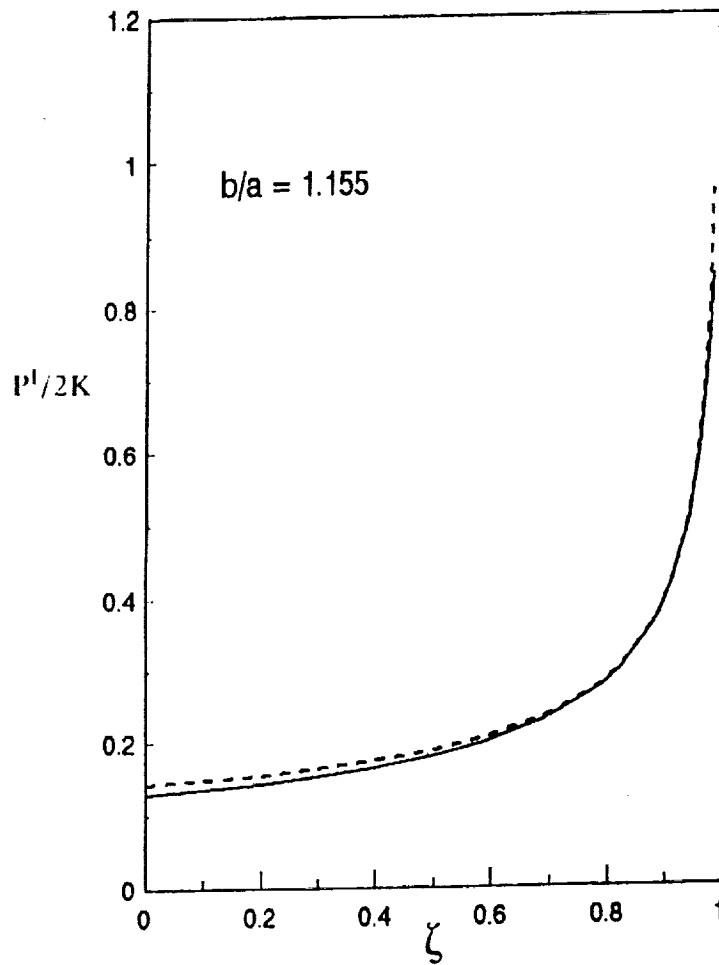
Fig.11 $P^l/2K$ vs. ζ for $b/a = 1.155$. Plane strain limit pressure and plane stress upper bound (dotted). Plane stress lower bound (solid).
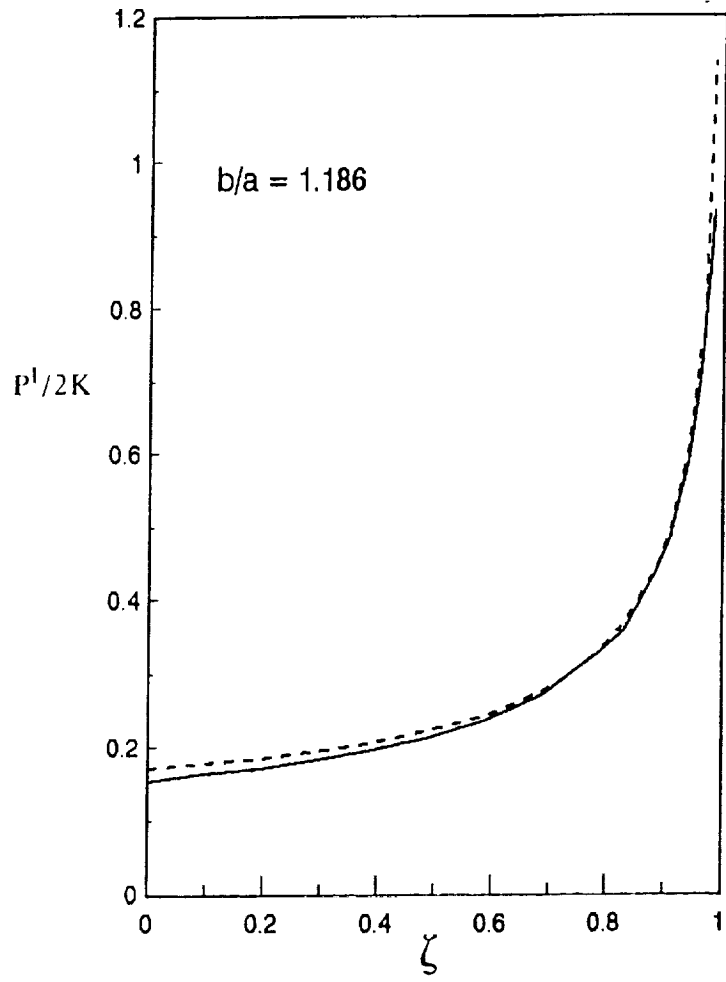
Fig.12 $P^l/2K$ vs. ζ for b/a = 1.186. Plane strain limit pressure and plane stress upper bound (dotted). Plane stress lower bound (solid).

REPORT DOCUMENTATION PAGE	*Form Approved* OMB No. 0704-0188

1. AGENCY USE ONLY *(Leave blank)*	2. REPORT DATE October 1991	3. REPORT TYPE AND DATES COVERED Final Contractor Report

4. TITLE AND SUBTITLE
Limit Pressure of a Circumferentially Reinforced SiC/Ti Ring

5. FUNDING NUMBERS
WU–510–01–50
G–NAG3–379

6. AUTHOR(S)
D.N. Robinson and M.S. Pastor

7. PERFORMING ORGANIZATION NAME(S) AND ADDRESS(ES)

University of Akron
Department of Civil Engineering
Akron, Ohio 44325–3905

8. PERFORMING ORGANIZATION REPORT NUMBER

None

9. SPONSORING/MONITORING AGENCY NAMES(S) AND ADDRESS(ES)

National Aeronautics and Space Administration
Lewis Research Center
Cleveland, Ohio 44135–3191

10. SPONSORING/MONITORING AGENCY REPORT NUMBER

NASA CR–187211

11. SUPPLEMENTARY NOTES
Project Manager, Steven M. Arnold, Structures Division, NASA Lewis Research Center, (216) 433–3334.

12a. DISTRIBUTION/AVAILABILITY STATEMENT

Unclassified - Unlimited
Subject Category 39

12b. DISTRIBUTION CODE

13. ABSTRACT *(Maximum 200 words)*
Limit loads under plane stress and plane strain are found for a circumferentially reinforced elastic-plastic ring subjected to interior pressure. These are used as bounds on an estimate of the failure pressure of a SiC/Ti test rig that is being fabricated and tested under the co-sponsorship of NASA Lewis Research Center and Pratt and Whitney Aircraft. The ring is to serve as a benchmark against which deformation and failure analysis methods can be assessed. An anisotropic perfect plasticity idealization of the SiC/Ti ring material is made and used in the limit load calculations. An estimate of the failure pressure of the NASA/PW benchmark test ring is given.

14. SUBJECT TERMS
Limit load; Anisotropic; Perfect plasticity; Metal matrix composite; Continuum mechanics

15. NUMBER OF PAGES
26

16. PRICE CODE
A03

17. SECURITY CLASSIFICATION OF REPORT	18. SECURITY CLASSIFICATION OF THIS PAGE	19. SECURITY CLASSIFICATION OF ABSTRACT	20. LIMITATION OF ABSTRACT
Unclassified	Unclassified	Unclassified	